Shot noise in GW detectors

G González

The dark fringe

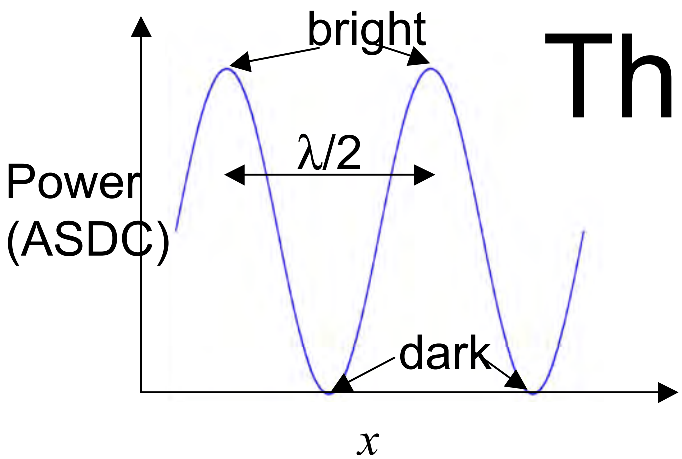

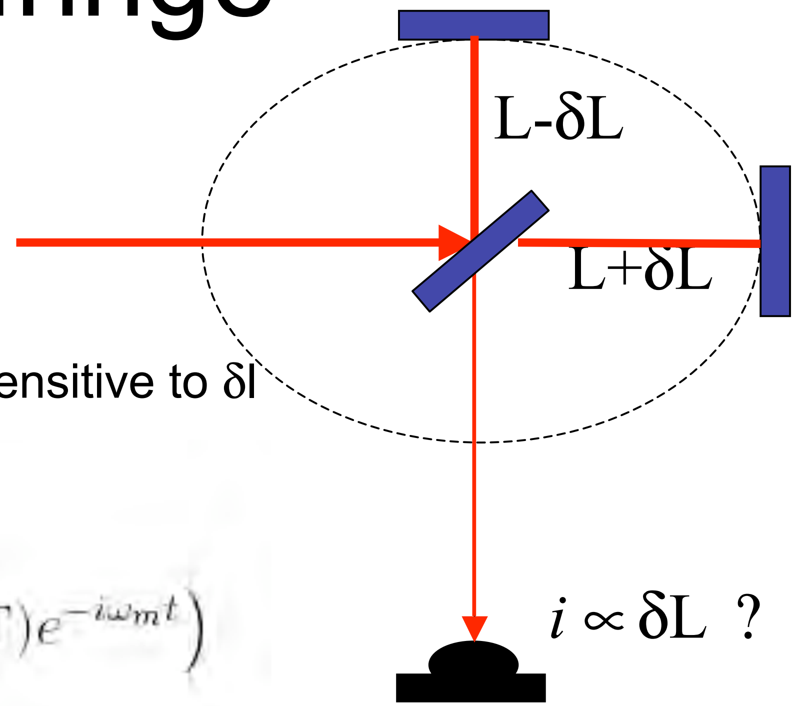

$P=P_0 \sin^2(\omega t+k\delta l) = (P_0/2)(1+\sin(2\omega t+2k\delta l))$: insensitive to δl

If we **phase-modulate** the light:

$$
\begin{aligned}
E &= E_0 e^{i(\omega t+\Gamma \sin(\omega_m t))} \\
&\approx E_0 e^{i\omega t}\left(J_0(\Gamma)+J_1(\Gamma)e^{i\omega_m t}-J_1(\Gamma)e^{-i\omega_m t}\right)
\end{aligned}
$$

For ω_m=25 MHz (λ_m=12 m), sidebands have w±wm=w0(1 ± 1.4 10^{-8}).

- If the Michelson arms are equal length in average, power is same (dark) for carrier and sidebands: no signal yet.
- If arms are not equal (**Schnupp asymmetry**), carrier is dark, but sidebands are not.
- The "beat" of carrier and sidebands has then a signal (photocurrent):

$P=|E_0+E_++E_-|^2 \propto DC + J_0J_1\sin(k\delta L)\sin(k_m DL)\sin(w_m t) + \ldots(2w_m t)$

- Then, "**demodulate**" : multiply by $\sin(w_m t)$ or $\cos(w_m t)$ to produce I and Q phases

Michelson interferometer

Shot noise at output : white noise with psd:

$$\phi^2(f) = 2\frac{h\nu}{\eta P}$$

Output signal:

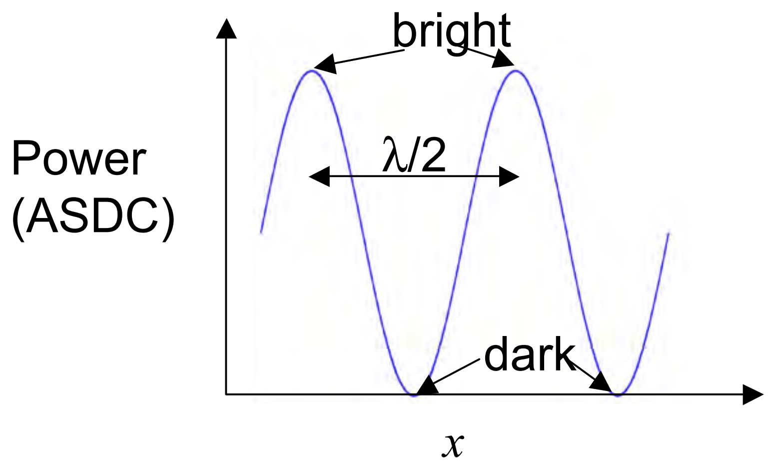

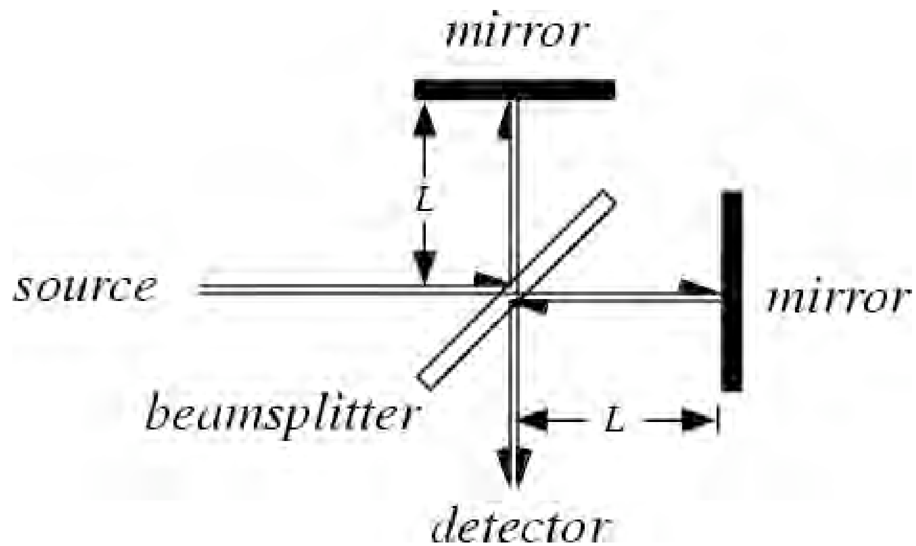

Power-recycled Michelson: PNI experiment 1995-1999

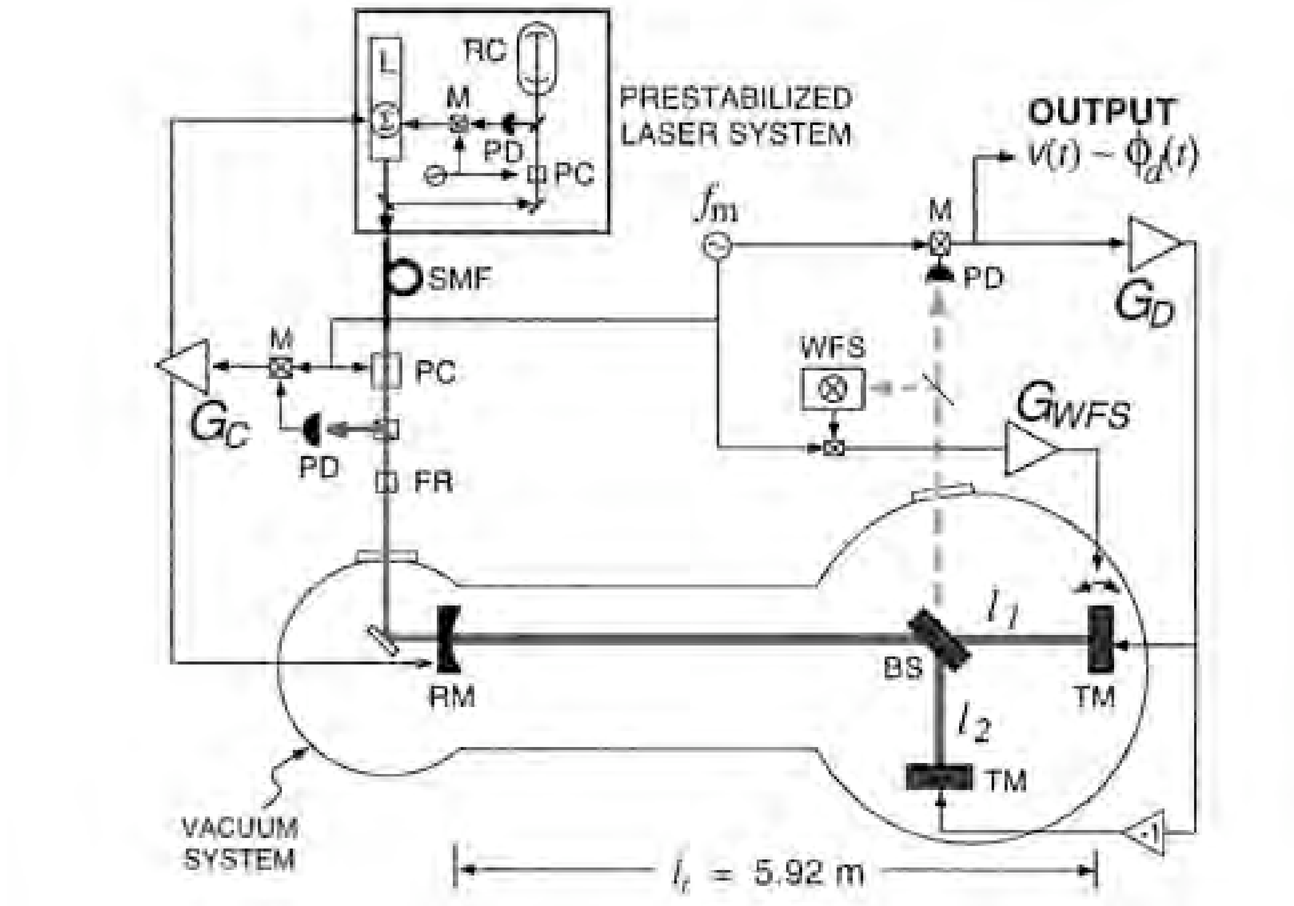

(green) PNI experiment

PRL, 80, p8131, 1998

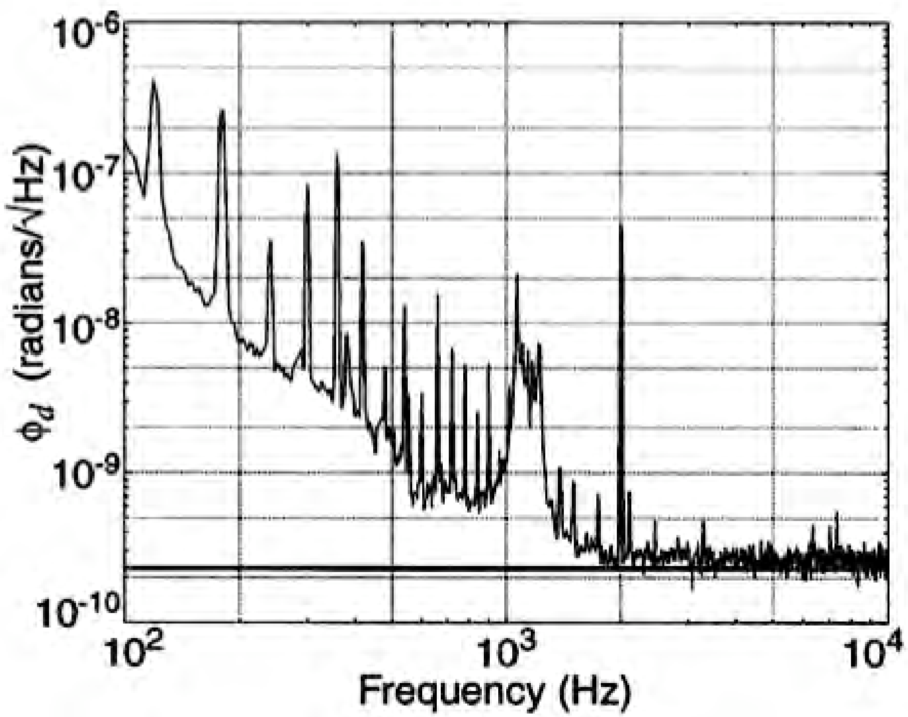

Lossless, mid fringe:

$$\phi^2(f) = \sqrt{2\frac{h\nu}{\eta P}}$$

Lossless, demodulated at dark fringe:

$$\phi^2(f) = F_{ns}\sqrt{2\frac{h\nu}{\eta P}} = \sqrt{3\frac{h\nu}{\eta P}}$$

Lossy, demodulated at dark fringe:

$$\tilde{\phi}_d(f) = F_{\rm ns}\sqrt{\frac{2h\nu_l}{\eta P_{\rm bs}}\left(1 + \frac{1-C}{4\sin^2(2k_m\Delta l)}R_{\rm bs}\right)},$$

Power-recycled Fabry Perot Michelson interferometer

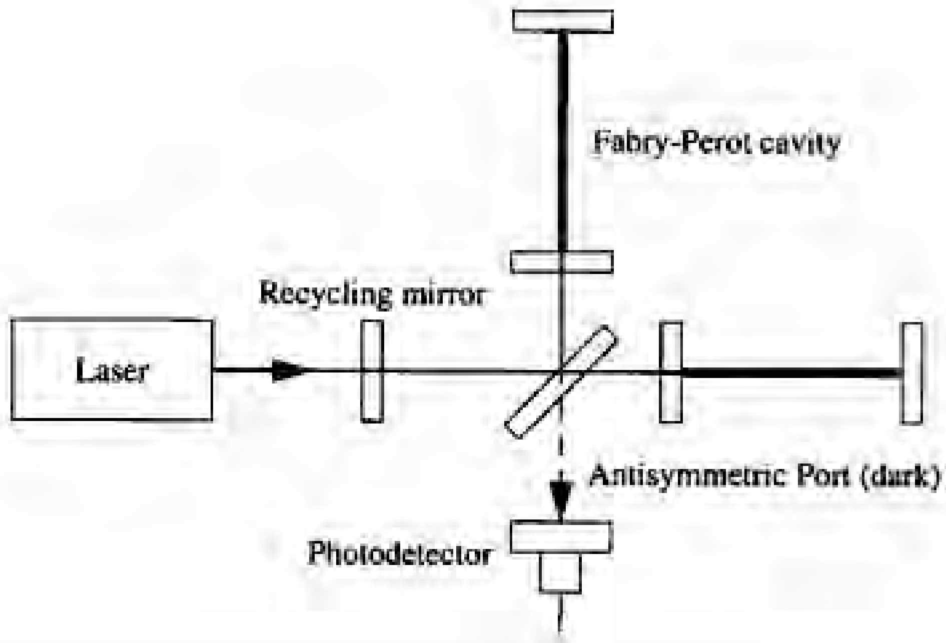

Fabry Perot cavity

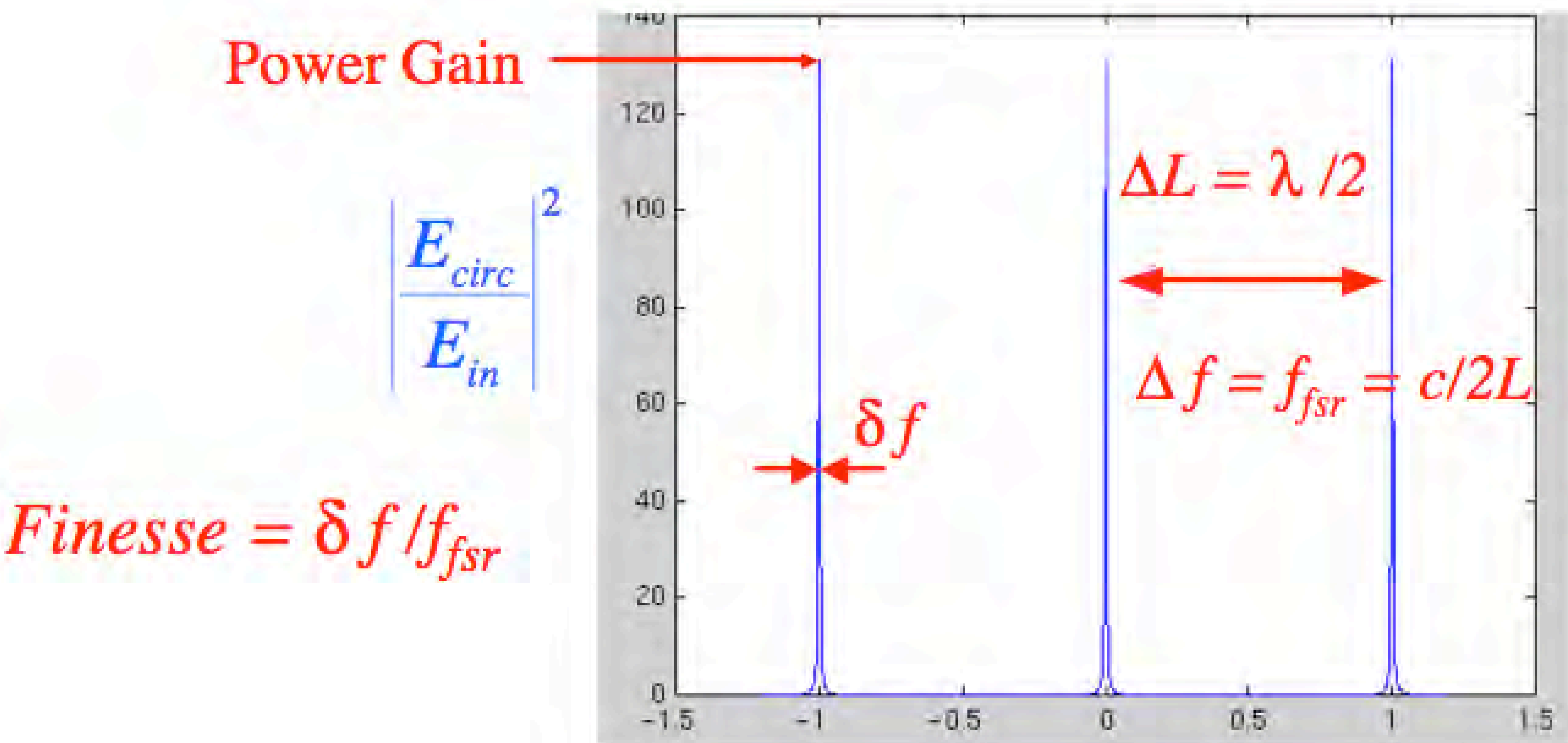

LIGO cavity parameters

- Finesse: peak separation / full width of peak
- Finesse = $F = \dfrac{\pi\sqrt{r_1 r_2}}{1 - r_1 r_2}$ = 208 for LIGO 4km arms
- Light storage time = $\tau_{stor} = \dfrac{L}{c}\dfrac{\sqrt{r_1 r_2}}{(1 - r_1 r_2)}$ = 870 μsec for LIGO arms
- Cavity pole = $f_{pole} = 1/(4\pi\tau_{stor})$ = 91 Hz for LIGO arms
- Cavity gain = $G_{cav} = \left(\dfrac{t_1}{1 - r_1 r_2}\right)^2$ = 130 for LIGO arms
- Visibility: $V = 1 - P_{min}/P_{max}$, Power in/out of lock
- LIGO 4km arms: $t_1^{\,2} = 0.03$, $r_2^{\,2} \approx 0.99997$

L1 “noise budget”

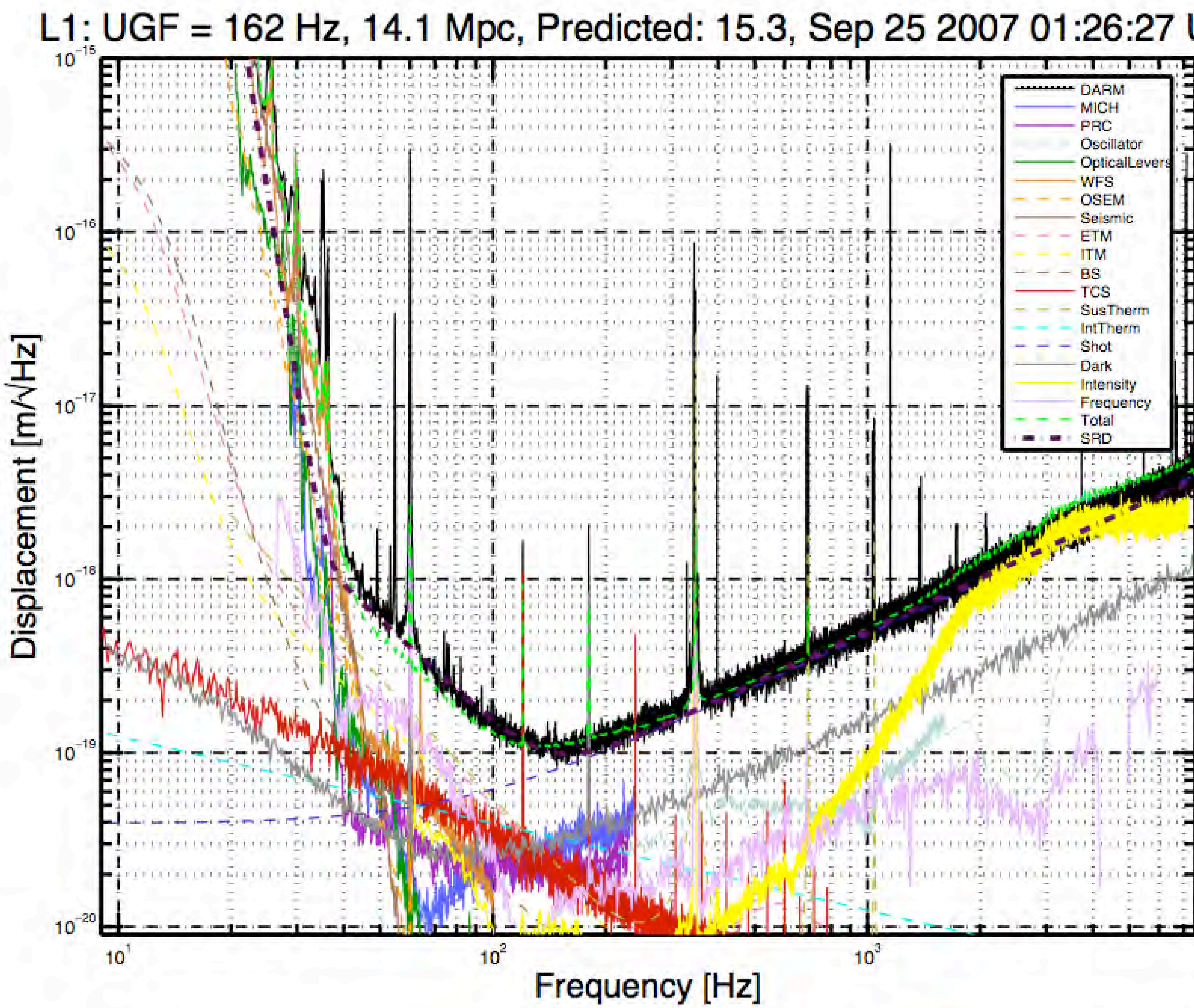

$\delta\phi \sim 4\pi\delta x/\lambda$

~1e-12 rad/rtHz

Shot noise and radiation pressure

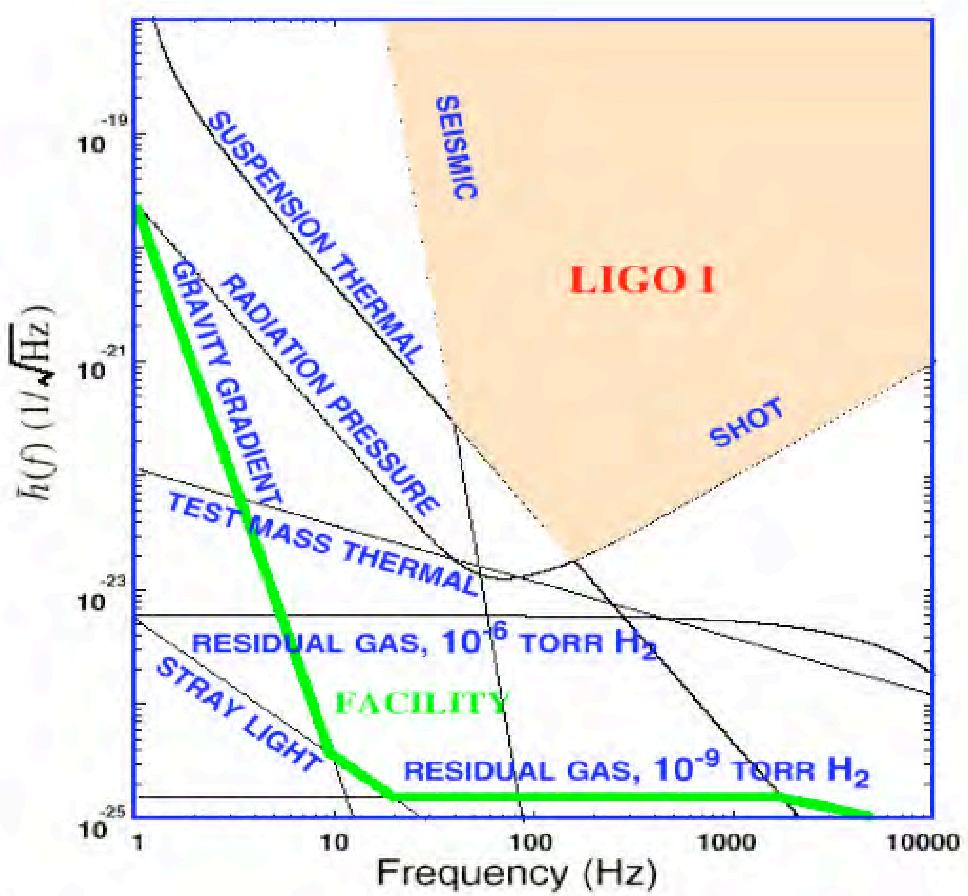

Standard quantum limit:

$$S_{SQL}(\omega) = \frac{4h}{\pi m \omega^2}$$

Advanced LIGO: signal recycling

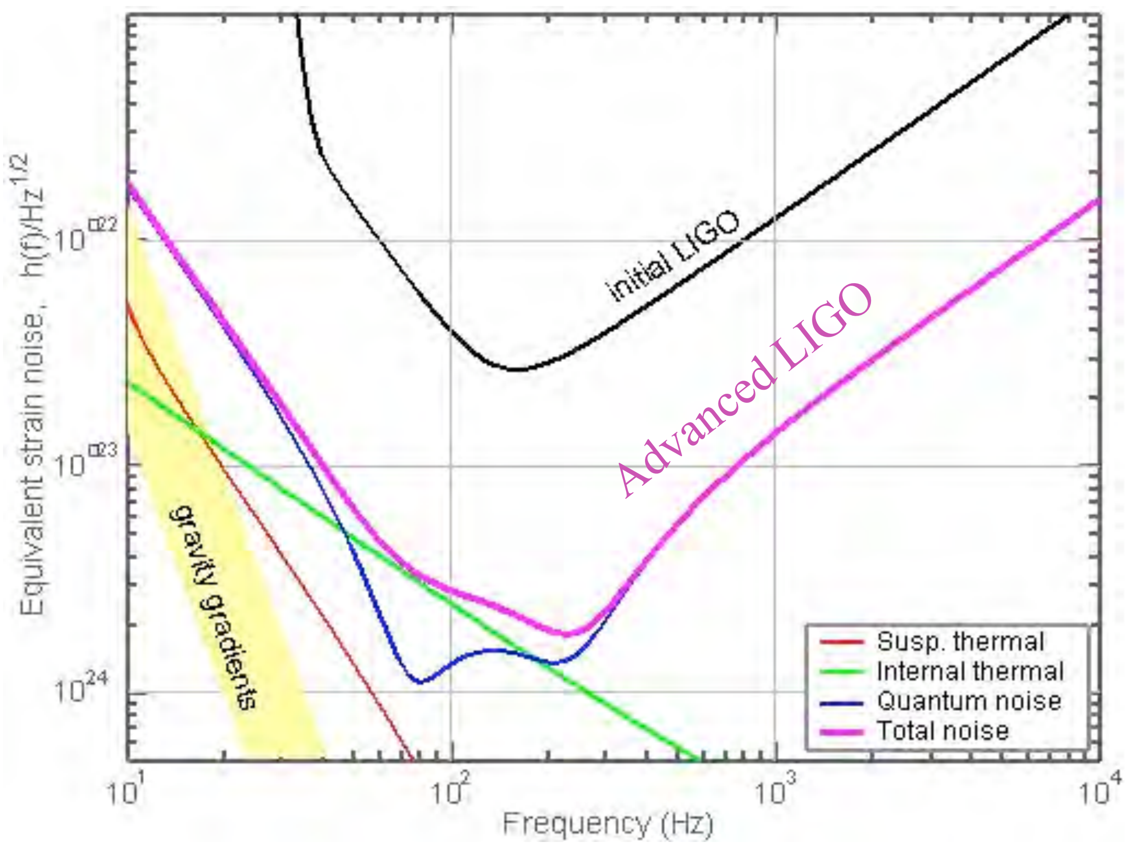

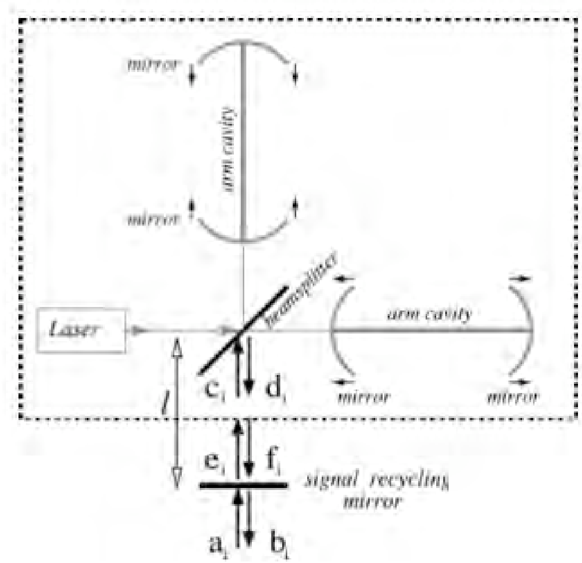

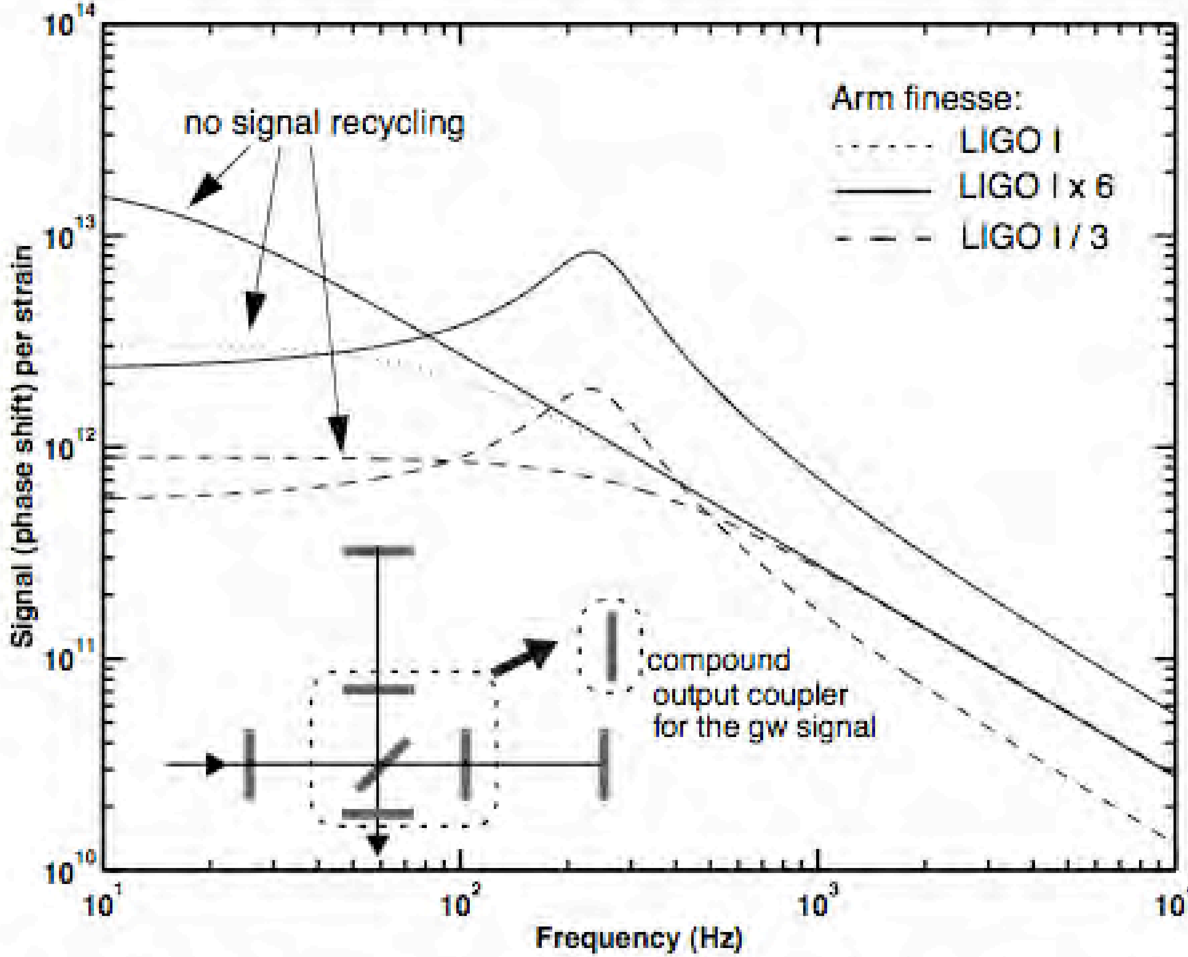

Figure 3: Interferometer gravitational-wave response curves with and without signal recycling. Shown is the optical phase shift per strain for three values of arm finesse: same as LIGO I; 6x the LIGO I finesse; 1/3 of the LIGO I finesse. For the latter two arm finesses, a response curve with signal recycling is shown; the high arm finesse signal recycled curve corresponds to the nominal LIGO II design, and the other curve illustrates that the same response shape can be obtained with a different arm finesse, by adjusting the signal mirror parameters. The low arm finesse signal recycled case has a overall smaller response, but this is compensated by the fact that the beamsplitter power would be higher, in theory yielding the same sensitivity for these two cases. In practice, nonlinear thermal lensing losses favor the design with higher arm finesse and lower beamsplitter power.

Beyond SQL

ALESSANDRA BUONANNO AND YANBEI CHEN

PHYSICAL REVIEW D **64** 042006

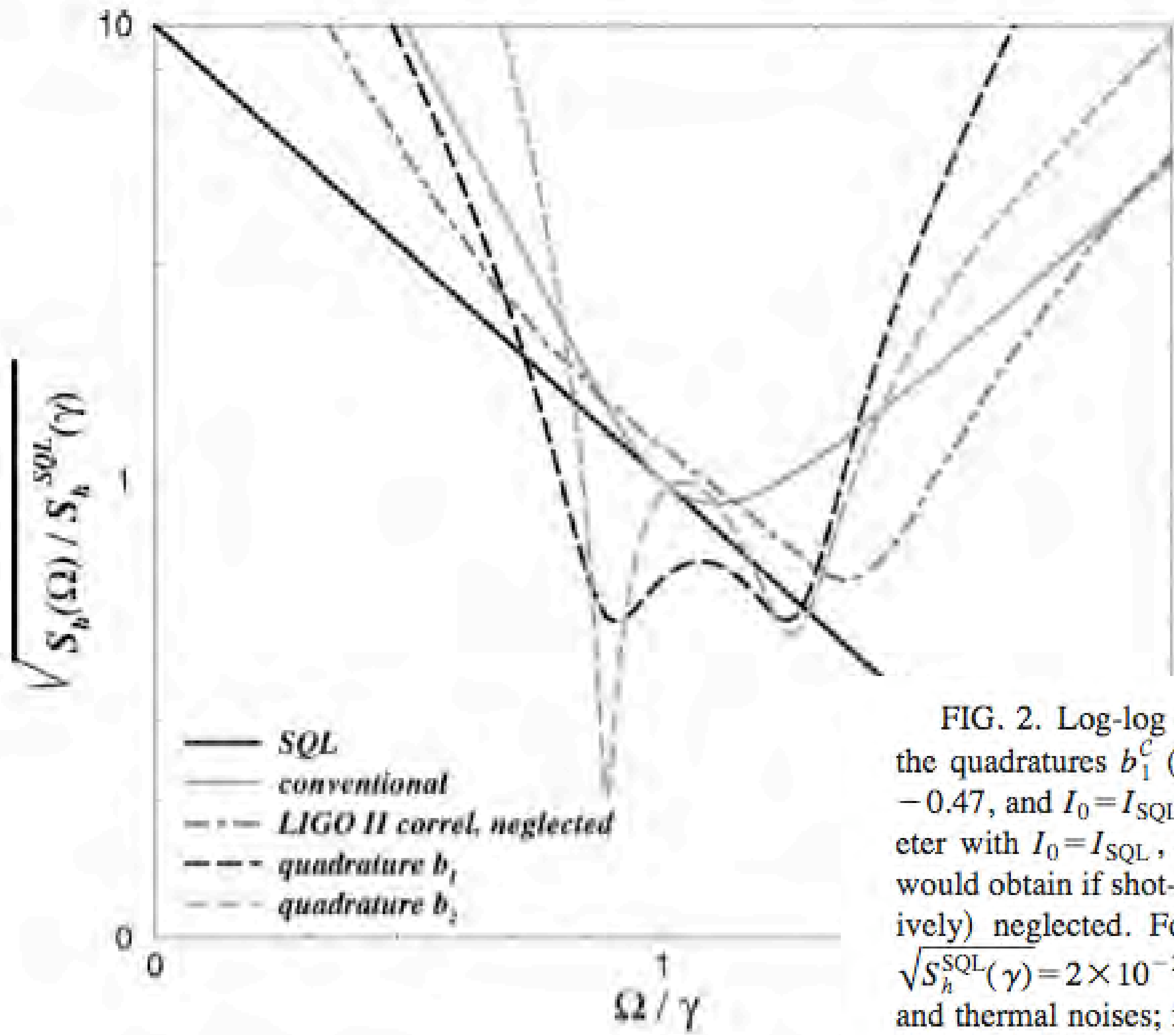

FIG. 2. Log-log plot of $\sqrt{S_h(\Omega)}/\sqrt{S_h^{\rm SQL}(\gamma)}$ versus Ω/γ for (i) the quadratures b_1^C ($\zeta=\pi/2$) and b_2^C ($\zeta=0$) with $\rho=0.9$, $\phi=\pi/2-0.47$, and $I_0=I_{\rm SQL}$, (ii) the SQL, (iii) a conventional interferometer with $I_0=I_{\rm SQL}$, and (iv) the noise curve of LIGO-II [21] one would obtain if shot-noise–radiation-pressure correlations were (naively) neglected. For LIGO-II, $\gamma=2\pi\times 100$ Hz (top axis) and $\sqrt{S_h^{\rm SQL}(\gamma)}=2\times 10^{-24}\ {\rm Hz}^{-1/2}$. These curves do not include seismic and thermal noises; for LIGO-II the latter is expected to be slightly above the SQL [15].

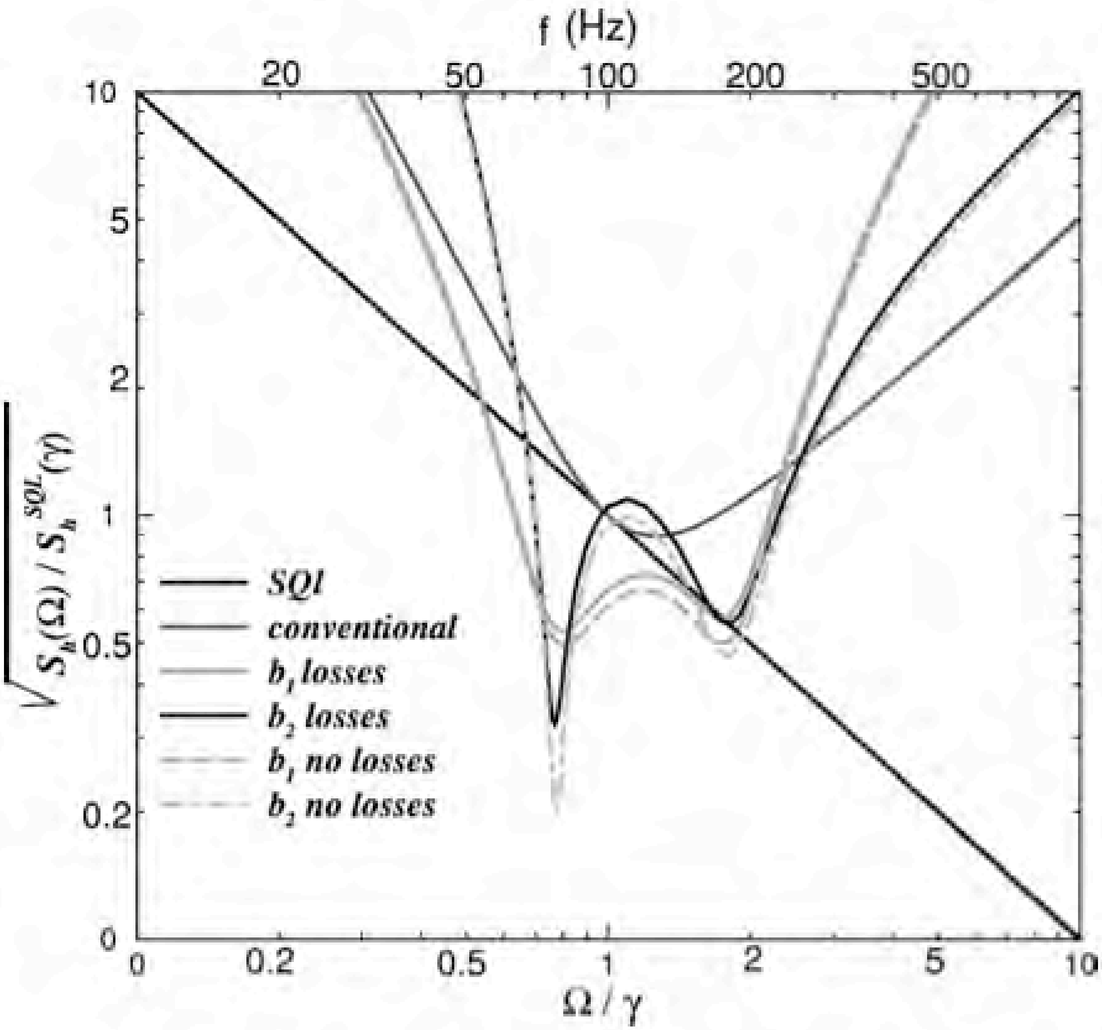

FIG. 8. Log-log plot of $\sqrt{S_h(\Omega)/S_h^{\mathrm{SQL}}(\gamma)}$ versus Ω/γ for the two quadratures b_1 ($\zeta=\pi/2$) and b_2 ($\zeta=0$), including and not including losses, with $\rho=0.9$, $\phi=\pi/2-0.47$, $I_0=I_{\mathrm{SQL}}$, $\epsilon=0.01$, $\lambda_{\mathrm{SR}}=0.02$ and $\lambda_{\mathrm{PD}}=0.1$. The noise curve for a conventional interferometer and the SQL are shown as well.

The references I used, in chronological order, were:

VOLUME 80, NUMBER 15 P H Y S I C A L R E V I E W L E T T E R S 13 APRIL 1998
High Power Interferometric Phase Measurement Limited by Quantum Noise
and Application to Detection of Gravitational Waves
P. Fritschel, G. González,* B. Lantz, P. Saha,† and M. Zucker

Shot noise in gravitational-wave detectors with
Fabry–Perot arms
Torrey T. Lyons, Martin W. Regehr, and Frederick J. Raab
20 December 2000 Vol. 39, No. 36 APPLIED OPTICS

Quantum noise in second generation, signal-recycled laser interferometric
gravitational-wave detectors
Alessandra Buonanno and Yanbei Chen
PHYSICAL REVIEW D, VOLUME 64, 042006

Second generation instruments for the Laser Interferometer
Gravitational Wave Observatory (LIGO)
Peter Fritschel
SPIE Proceedings
LIGO document P020016-00.pdf
http://www.ligo.caltech.edu/docs/P/P020016-00.pdf